

# GAMMA-RAY BURST AFTERGLOW WITH CONTINOUS ENERGY INJECTION: SIGNATURE OF A HIGHLY-MAGNETIZED MILLISECOND PULSAR

BING ZHANG & PETER MÉSZÁROS

Astronomy & Astrophysics Dept., Pennsylvania State University, University Park, PA 16802

*Draft version December 2, 2024*

## ABSTRACT

We investigate the possible consequences of a continuously injecting central engine on the Gamma-Ray Burst afterglow emission, focusing more specifically on the possibility that the central source is a highly-magnetized millisecond pulsar. If the initial parameters of the pulsar are within a certain region of the surface field - rotation period parameter space, the burst afterglow lightcurves are predicted to show a distinctive achromatic bump or break feature, the onset and duration of which range from minutes to months, depending on the pulsar and the fireball parameters. The detection of or upper limits on such features would provide constraints on the possible progenitor, and on magnetar-like central engine models. An achromatic bump such as that observed in GRB 000301C afterglow may be attributed to a millisecond pulsar with  $P_0 = 7\text{ms}$  and  $B_p = 5.5 \times 10^{14} \text{ G}$ .

*Subject headings:* gamma rays: bursts - radiation mechanisms: nonthermal - pulsars: general - magnetic fields

## 1. INTRODUCTION

Much of the current research on Gamma-ray bursts (GRB) is proceeding along two major directions. One is trying to understand how a large amount of bulk kinetic energy in an explosive outflow is converted into radiation and the other is trying to determine the nature of the central engine and its progenitor, which powers the whole event. The theory for the former, which invokes relativistic fireballs and shocks is relatively developed, although many uncertainties remain, while investigations on the latter have only recently started to yield substantial results, and evidence for likely progenitors is still tentative. Thus, the investigation of criteria to differentiate between various central engine possibilities is desirable.

The fireball shock model has provided satisfactory interpretations of the afterglows observed from a number of GRBs (e.g. Wijer, Rees & Mészáros 1997; Vietri 1997; Chevalier & Li 1999; Sari & Piran 1999). Almost all of these models assume prompt injection of GRB energy into the fireball, including those considering various “post-standard” non-uniform injection features (e.g., Mészáros, Rees & Wijer 1998), including the “refreshed shock” scenario (Rees & Mészáros 1998; Sari & Mészáros 2000). However, in some types of central engines, such as a fast-rotating high-field pulsar (magnetar) or a black hole plus a long-lived debris torus system, a significant energy input into the fireball may in principle continue for a time scale significantly longer than the  $\gamma$ -ray emission. Therefore, there is a need to investigate a continuously-fed fireball in more detail. An additional motivation is provided by the recent detection of Fe features in the X-ray afterglow of GRB 991216 after about 1.5 days (Piro et al. 2000) and GRB 000214 after about 1 day (Antonelli et al, 2000), which may require a continuing post-burst outflow in order to achieve less restrictive Fe abundance constraints (Rees & Mészáros , 2000). Dai & Lu (1998a,b) have considered continuous injection from a millisecond (although not high-field) pulsar to interpret the afterglow light curve of

some GRBs, but did not perform a systematic study of this topic. In this paper, we investigate the observational consequences of a continuously injecting central engine, and more specifically, focus on the possibility that the central engine is a millisecond pulsar, in particular a highly magnetized pulsar or magnetar.

## 2. CONTINOUS-INJECTION DYNAMICS

The differential energy conservation relation for a self-similar blast wave can be written in general form as  $dE/dt = \mathcal{L}_0(t/t_0)^q - \kappa(E/t)$ , where the first term on the right denotes a steady energy injection into the fireball, and the second term denotes the possibility of radiative energy losses of the fireball, with  $q$  and  $\kappa$  being dimensionless constants (Cohen & Piran 1999). Here  $t$  is measured in the burst frame, in which the radius of the relativistic shell is given by  $r = ct$ , and  $\mathcal{L} = \mathcal{L}_0(t/t_0)^q$  is the luminosity of the central engine measured with this time. For  $q \neq -1 - \kappa$ , an analytical solution is (Cohen & Piran 1999)

$$E = \frac{\mathcal{L}_0}{\kappa+q+1} \left( \frac{t}{t_0} \right)^q t + E_{\text{imp}} \left( \frac{t}{t_0} \right)^{-\kappa}, \quad t > t_0. \quad (1)$$

Here  $t_0$  is a characteristic timescale for the formation of a self-similar solution, which is roughly equal to the time for the external shock to develop as a result of deceleration by the external medium, and  $E_{\text{imp}}$  is a constant which describes the impulsive energy input when  $q > -1 - \kappa$  (see footnote 1). Eq.(1) is a solution under the assumption that a self-similar solution exists at  $t > t_0$ , hence it cannot be extrapolated down to  $t = 0$ , where there is no self-similar solution at all. Setting  $t = t_0$  in equ. (1) shows that formally the total energy at the beginning of the self-similar expansion may be considered as the sum of two terms,  $E_0 = \mathcal{L}_0 t_0 / (\kappa + q + 1) + E_{\text{imp}}$ . For  $q > -1 - \kappa$ , the first term is the accumulated energy from the continuous injection before the external shock has formed, while the second term,  $E_{\text{imp}}$ , is the energy injected impulsively by

the initial cataclysmic event<sup>1</sup>.

After the time  $t_0$  the bulk Lorentz factor of the fireball can be taken to scale with time as  $\Gamma^2 \propto t^{-m}$ , with  $m$  and  $\kappa$  connected by  $\kappa = m - 3$  (Cohen, Piran & Sari 1998), and  $m = 3$  for the adiabatic case (Blandford & McKee 1976). The burst-frame time  $t$  is related to the observer-frame time  $T$  through  $dT = (1 - \beta)dt \simeq dt/2\Gamma^2$ . The integrated transformation law between the two sets of times is then  $T = \int_0^t (2\Gamma^2)^{-1} dt = t/2(m+1)\Gamma^2$ . It is more convenient to express the energy equation in terms of the observer frame injection luminosity  $L$  and the observer time  $T$ . Equation (1) then reads

$$E = \left( \frac{m+1}{\kappa+q+1} \right) L_0 \left( \frac{T}{T_0} \right)^q T + E_{\text{imp}} \left( \frac{T}{T_0} \right)^{-\kappa}, \quad T > T_0 \quad (2)$$

where  $T_0 = t_0/2(m+1)\Gamma^2$ ,  $L = L_0(T/T_0)^q = 2\Gamma^2\mathcal{L}$ . We see that the total energy in the fireball includes the contributions from the injection term with a time dependence  $\propto T^{(q+1)}$  as well as an energy loss term with a time dependence  $\propto T^{-\kappa}$ . Which of these two terms is dominant at a particular observation time depends both on the relative values of the two indices ( $q+1$  and  $-\kappa$ , Cohen & Piran 1999), and also on the values of  $L_0$  and  $E_{\text{imp}}$  (Dai & Lu 1998a,b). We then have three regimes: 1. If  $q < -1 - \kappa$ , the second term in (1) and (2) always dominates since the first term is negative. (Recall that in this case the division in two such terms has no clear physical meaning). The fireball is then completely analogous to the impulsive injection case. 2. If  $q = -1 - \kappa$ , the solution (1) is no longer valid, and there is no self-similar solution (Cohen & Piran 1999). 3. If  $q > -1 - \kappa$ , the first term in (1) and (2) will eventually dominate over the second term after a critical time  $T_c$ , and it is this term that will exert a noticeable influence on the GRB afterglow light curves. This is the case we are interested in.

For a fireball being decelerated by a homogeneous external medium, generally the energy conservation equation at time  $t$  can be expressed as

$$E = \frac{4\pi}{3} r^3 n m_p c^2 \Gamma^2 = \frac{4\pi}{3} (\beta c t)^3 n m_p c^2 \Gamma^2, \quad t > t_0, \quad (3)$$

where  $n$  is the particle number density in the external medium,  $r$  is the radius of the external shock caused by the interaction of the fireball and the external medium, and all other symbols have their usual meanings. This relation does not depend on  $m$ , and holds also for more general cases with a non-constant  $E$ . For the injection dominated case, the first term in (2) should have the same time dependence as  $E$  in (3), i.e.,  $T^{q+1} \propto t^3\Gamma^2$ , giving (cf. Blandford & McKee 1976)

$$m = \frac{2-q}{2+q}, \quad q > -1 - \kappa. \quad (4)$$

This result does not depend on  $\kappa$ , because the energy loss term is negligible when the injection term dominates. Since in general  $\Gamma \propto r^{-m/2} \propto T^{-m/2(m+1)}$  and  $r \propto T^{1/(m+1)}$ , we can get the dynamical law of the injection-dominated case using (4),

$$\Gamma \propto r^{-(2-q)/2(2+q)} \propto T^{-(2-q)/8}, \quad r \propto T^{(2+q)/4}. \quad (5)$$

<sup>1</sup>For  $q < -1 - \kappa$ , the two terms above no longer have the clear physical meanings. Strictly speaking, the accumulated injection energy for  $q > -1 - \kappa$  is  $\mathcal{L}_0 t_0 / (q+1)$ , but usually  $\kappa \sim 0$  is a good approximation.

For a continuously-fed fireball, a forward shock propagating into the external medium, and a reverse shock propagating into the relativistic fireball will co-exist on either side of the contact discontinuity. The latter may persist as long as a significant level of energy injection is going on. The radiation spectra from these shocks are complicated by many factors. Here we address only the simplest case of the standard adiabatic external shock afterglow scenario, and assume that the reverse shock is mildly relativistic, as in the refreshed shock scenario. Following Mészáros & Rees (1997) and Sari & Mészáros (2000), one can work out the relationship between the temporal index  $\alpha$  and the spectral index  $\beta$ , where  $F_\nu \propto T^\alpha \nu^\beta$ . For the forward shock, the synchrotron peak-frequency decays as  $\nu_m^f \propto \Gamma B' \gamma_m^2 \propto \Gamma^4 \propto T^{-2m/(m+1)} \propto T^{-(2-q)/2}$ , and the peak flux evolves with time as  $F_{\nu_m}^f \propto n_e' B' r / \Gamma \propto T^3 \Gamma^8 \propto T^{(3-m)/(1+m)} \propto T^{1+q}$ , so that  $\alpha^f = (2m\beta^f + 3 - m)/(1+m) = (1 - q/2)\beta^f + 1 + q$ . For the reverse shock,  $\nu_m^r = \nu_m^f / \Gamma^2 \propto \Gamma^2 \propto T^{-m/(m+1)} \propto T^{-(2-q)/4}$ , and  $F_{\nu_m}^r = \Gamma F_{\nu_m}^f \propto T^3 \Gamma^9 \propto T^{(6-3m)/2(1+m)} \propto T^{(6+9q)/8}$ , so that  $\alpha^r = (2m\beta^r + 6 - 3m)/2(1+m) = [(4 - 2q)\beta^r + 9q + 6]/8$ . At a given time for a given frequency, the emission may be dominated either by the forward or the reverse shock. The above scalings assume that the synchrotron cooling frequency is above  $\nu_m$  (i.e. slow cooling regime, Sari, Piran & Narayan 1998), which is usually satisfied. The fast cooling will change the scaling laws above, but does not change the qualitative “switching” picture proposed in this paper. All the above scalings reduce to the “standard” adiabatic case by setting  $m = 3$  and  $q = -1$ .

A critical time  $T_c$  for the beginning of the injection-dominated regime can be defined by equating the injection term to the energy loss term in (2),

$$T_c = \text{Max} \left\{ 1, \left[ \left( \frac{\kappa+q+1}{m'+1} \right) \left( \frac{E_{\text{imp}}}{L_0 T_0} \right) \right]^{1/(\kappa+q+1)} \right\} T_0, \quad (6)$$

where  $m'$  is the scaling law before the injection law dominates, and  $T_c \geq T_0$  ensures that a self-similar solution has already formed when the injection law dominates. If initially the continuous injection term is more important, i.e.,  $L_0 T_0 \gtrsim E_{\text{imp}}$ , the critical time is essentially  $T_0$ , and the dynamics is determined by the continuous injection law as soon as the self-similar profile is formed. However, if initially the impulsive injection term dominates ( $L_0 T_0 \ll E_{\text{imp}}$ ), the critical time  $T_c$  after which the continuous injection becomes dominant could be much longer than  $T_0$ , depending on the ratio of  $E_{\text{imp}}$  and  $L_0 T_0$ .

Central engines endowed with this general type of behavior may, in addition, have another characteristic timescale  $\mathcal{T}$ , e.g. at which an injection power law index  $q > -1 - \kappa$  switches to a steeper value  $q < -1 - \kappa$ . It is only for cases with  $\mathcal{T} > T_c$  that the continuous injection law has a noticeable effect on the afterglow light curve. Different central engines may have different characteristic values of  $\mathcal{T}$ . In the following, we consider the specific case of a millisecond pulsar as the central engine, and investigate the conditions under which a continuous injection law can influence the dynamics of the blast wave.

### 3. HIGHLY MAGNETIZED MILLISECOND PULSAR AS THE CENTRAL ENGINE

Although a wide range of GRB progenitors lead to a black hole - debris torus system (Woosley 1993; Paczyński 1998; Mészáros, Rees & Wijers 1999; Fryer, Woosley & Hartmann 1999), some progenitors may lead to the formation of a highly-magnetized rapidly rotating pulsar (e.g. Usov 1992; Duncan & Thompson 1992; Thompson 1994; Yi & Blackman 1998; Blackman & Yi 1998; Kluźniak & Ruderman 1998; Spruit 1999; Ruderman, Tao & Kluźniak 2000). During the early stages of the evolution of these central objects, the luminosity decay law could be very complicated. On the longer (afterglow) timescales that we are interested in, some short-term processes, such as the decay of the differential-rotation-induced toroidal magnetic field energy (Kluźniak & Ruderman 1998; Ruderman et al. 2000), are no longer important, and the substantial energy injection into the fireball may be mainly through electromagnetic dipole emission. The spindown behavior of the pulsar, which is essential for the dipolar injection law, may be also influenced by gravitational radiation and by the outflowing wind. To be important, central-engine pulsars generally need to rotate with millisecond-order periods, so the light cylinders are very close in and the wind spindown (e.g. Harding, Contopoulos & Kazanas 1999) may be not important. The energy input from these winds (e.g. Alfvén waves, Thompson & Blaes 1998) is also likely to be small compared to the dipole luminosity, although it may be important for the slow magnetars conjectured to interpret the soft gamma-ray repeaters.

Assuming that the spindown is mainly due to electromagnetic dipole emission and to gravitational radiation, the spindown law is  $-I\Omega\dot{\Omega} = (B_p^2 R^6 \Omega^4)/(6c^3) + (32GI\epsilon^2\Omega^6)/(5c^5)$  (Shapiro & Teukolsky 1983), where  $\Omega$  and  $\dot{\Omega}$  are the angular frequency and its time derivative,  $B_p$  is the dipolar field strength at the magnetic poles,  $I$  is the moment of inertia,  $R$  is the stellar radius,  $\epsilon$  is ellipticity of the neutron star (assuming a slightly deformed homogeneous ellipsoid). This equation can be solved for  $\Omega$  as a function of  $T$ , with initial conditions  $\Omega = \Omega_0$ ,  $\dot{\Omega} = \dot{\Omega}_0$  for  $T = 0$ . The energy input into the fireball is due to the dipole emission (since the gravitational radiation can escape freely). Thus, the solution  $\Omega(T)$  can be used to write the continuous energy injection into the fireball as  $L(T) = [B_p^2 R^6 \Omega(T)^4]/(6c^3)$ , which is usually not a simple power-law. However, the spindown will be dominated by one of the two terms over different time regimes, and one can get approximate solutions for these two regimes. When electromagnetic dipole radiation (EMDR) losses dominate the spindown, we have  $\Omega = \Omega_0(1 + T/\mathcal{T}_{em})^{-1/2}$ , or approximately  $\Omega = \Omega_0$  for  $T \ll \mathcal{T}_{em}$ , and  $\Omega = \Omega_0(T/\mathcal{T}_{em})^{-1/2}$  for  $T \gg \mathcal{T}_{em}$ . Here

$$\mathcal{T}_{em} = \frac{3c^3 I}{B_p^2 R^6 \Omega_0^2} = 2050 \text{ s } I_{45} B_{p,15}^{-2} P_{0,-3}^2 R_6^6, \quad (7)$$

is the characteristic time scale for the dipole spindown,  $B_{p,15} = B_p/(10^{15}\text{G})$ , and  $P_{0,-3}$  is the initial rotation period in milliseconds. On the other hand, when gravitational wave radiation (GWR) losses dominate the spindown, the evolution can be written as  $\Omega = \Omega_0(1 + T/\mathcal{T}_{gw})^{-1/4}$  where  $\mathcal{T}_{gw} = (5c^5/128GI\epsilon^2\Omega_0^4) =$

0.91 s  $I_{45}^{-1} P_{0,-3}^4 (\epsilon/0.1)^{-2}$ . According to Usov (1992) and Blackman & Yi (1998), gravitational radiation spindown is important only when  $\Omega_0$  is greater than a critical value,  $\Omega_* \sim 10^4 \text{s}^{-1}$ . In such cases the ellipticity is large ( $\epsilon \sim 0.1$ ) due to neutron star rotation instability, and the timescale for the GWR-dominated regime is short, so that  $\Omega$  will be damped to below  $\Omega_*$  promptly after in a time  $\mathcal{T}_* = [(\Omega_0/\Omega_*)^4 - 1]\mathcal{T}_{gw}$ . After  $\Omega < \Omega_*$ , gravitational radiation losses decrease sharply, and the spindown behavior is determined by the electromagnetic dipole radiation. If the neutron star is born with  $\Omega_0 < \Omega_*$ , the spindown history will be always in the EMDR regime, since the typical spindown time for gravitational radiation is much longer (e.g. for typical ellipticities as in the Crab pulsar,  $\epsilon \sim 3 \times 10^{-4}$ ).

The continuous injection luminosity in above two cases are

(A)  $\Omega_0 < \Omega_*$ : This is the relatively simple case where EMDR losses dominate. The injection luminosity is

$$L(T) = L_{em,0} \frac{1}{(1+T/\mathcal{T}_{em})^2} \simeq \begin{cases} L_{em,0}, & T \ll \mathcal{T}_{em} \\ L_{em,0} \left(\frac{T}{\mathcal{T}_{em}}\right)^{-2}, & T \gg \mathcal{T}_{em}, \end{cases} \quad (8)$$

where  $\mathcal{T}_{em}$  is given by (7), and

$$L_{em,0} = \frac{I\Omega_0^2}{2\mathcal{T}_{em}} \simeq 10^{49} \text{ erg s}^{-1} B_{p,15}^2 P_{0,-3}^{-4} R_6^6. \quad (9)$$

(B)  $\Omega_0 > \Omega_*$ : The injection luminosity can be divided into two phases, i.e.,  $L = L_{em,0}/(1 + T/\mathcal{T}_{gw})$  for  $T < \mathcal{T}_*$  or  $L = L_{em,c}/[1 + (T - \mathcal{T}_*)/\mathcal{T}_{em}]^2$  for  $T > \mathcal{T}_*$ , where  $L_{em,0}$  is given by (9), and  $L_{em,*} = I\Omega_*^2/2\mathcal{T}_{em,*} \simeq 10^{49} \text{ erg s}^{-1} B_{p,15}^2 P_{*,-3}^{-4} R_6^6$ , where  $\mathcal{T}_{em,*} = 3c^3 I/B_p^2 R^6 \Omega_*^2 \simeq 2050 \text{ s } I_{45} B_{p,15}^{-2} P_{*,-3}^2 R_6^6$ .

The above injection luminosities have, for certain time regimes, a temporal index  $q = 0 > -1$ , which may potentially dominate the blast wave dynamics. The typical duration times for this flat injection law are  $\mathcal{T}_{em}$  for case (A) or  $\mathcal{T}_{gw}$  and  $(\mathcal{T}_* + \mathcal{T}_{em,*})$  for case (B). In case (B) there are two luminosity “plateaus”. The former is usually much shorter than  $T_c$  unless a very dense medium is assumed (see below), so it is unlikely to detect such a “two-step” injection-dominated case. If  $\Omega_*$  is close to  $\Omega_0$ , the second timescale for case (B), i.e.,  $(\mathcal{T}_* + \mathcal{T}_{em,*})$ , may not be much different from  $\mathcal{T}_{em}$ . In the following, for simplicity, we will discuss case (A) only, keeping in mind the possible extra complexity which case (B) may introduce in some extreme cases.

The time interval  $T_c < T < \mathcal{T}_{em}$  is the regime where one can expect a distinctive pulsar feature to show up in the lightcurve. We take as an example the behavior (8), setting  $q = 0$  in this regime, and  $q = -1$  otherwise (since the second slope  $q = -2$  would mimick in effect the standard impulsive  $q = -1$ ,  $m = 3$  adiabatic case). For the slow-cooling standard external shock scenario discussed in §2, we can get then the switch in behavior of the temporal decay index. This switches from  $\alpha_1$  to  $\alpha_2 = (2/3)\alpha_1 + 1$  at  $T_c$ , and switches back to  $\alpha_1$  again at  $\mathcal{T}_{em}$ . The temporal index in this approximation is related to the spectral slope  $\beta$  through  $\alpha_1 = (3/2)\beta$  for the forward-shock-dominated case, and  $\alpha_1 = (6\beta - 3)/8$  for the reverse-shock-dominated

case. This implies an *acromatic* bump in the light curve, which could provide a direct signature for the existence of a pulsar. However, not all millisecond pulsars would give such observable features. The condition for detecting the above continuous injection features is  $T_{em} > T_c$ , which constrains the phase space of the initial parameters of the pulsar at birth. Let us specify the pulsar case, i.e.,  $q = 0$ , and further assume  $\kappa = 0$ ,  $m' = 3$ , so Eq.(6) is simplified to  $T_c = \text{Max}(1, E_{\text{imp}}/4L_0 T_0) T_0$ . This gives two regimes:

(I)  $E_0$  is mainly due to the continuous injection, i.e.,  $E_{\text{imp}} \lesssim 4L_0 T_0$ . This is the case considered in many pulsar GRB central engine models (Usov 1992; Duncan & Thompson 1992; Thompson 1994; Spruit 1999). We then have  $T_c = T_0$  and  $E_0 \simeq 4L_{em,0} T_0$  (a factor of 2 if the continuous injection and the prompt injection energies are comparable). Solving  $E_0 = (4\pi/3)(8c\Gamma_0^2 T_0)^3 n m_p c^2 \Gamma_0^2$ , where  $\Gamma_0 = E_0/\Delta M$  is the initial bulk Lorentz factor of the blast wave, we have  $T_c = T_0 \simeq 6.7s B_{p,15} P_{0,-3}^{-2} R_6^3 \Gamma_{0,2}^{-4} n^{-1/2}$ . The condition  $T_{em} > T_0$  then implies

$$B_{p,15} < 6.8 P_{0,-3}^{4/3} R_6 I_{45}^{1/3} \Gamma_{0,2}^{4/3} n^{1/6}. \quad (10)$$

(II)  $E_0$  is dominated by the impulsive injection. This could be the case when a pulsar is associated with the GRB, but some additional impulsive energy is required to power the GRB (e.g. the differentially-rotating neutron star model, Ruderman et al. 2000, or the phase conversion model from a neutron star to a strange star, Dai & Lu 1998b). In this case, since  $E_{\text{imp}} > 4L_0 T_0$ , we have  $T_c = E_{\text{imp}}/4L_{0,em} = (E_{\text{imp}}/2I\Omega_0^2) T_{em}$ . The condition  $T_{em} > T_c$  is simply  $E_{\text{imp}} < 2I\Omega_0^2$ , which reads

$$P_{0,-3} < 8.9 I_{45}^{1/2} E_{\text{imp},51}^{-1/2}. \quad (11)$$

Since both  $T_{em}$  and  $T_c$  are large in this case, the continuous injection term may dominate at a later time.

In addition, to avoid rotational break-up of the pulsar

$$P_0 > P_0(\text{min}) \quad (12)$$

is required. The lines defined by equation (10), (11) and (12) then define a region in the  $P_0, B_{p,0}$  initial parameter space of the pulsar, inside which the continuous injection has the observational signature discussed above (see Fig.1). The separation between the two regimes may be defined by the condition  $4L_{em,0} T_0 \simeq 10^{51} E_{\text{imp},51}$  erg, or  $B_{p,15} \simeq 1.6 P_{0,-3}^2 R_6^{-3} \Gamma_{0,2}^{4/3} n^{1/6} E_{\text{imp},51}^{1/2}$ . Above this line (I), since  $T_c = T_0$  one expects only one switch, starting with the flat regime and switching to steep; below this line (II) one expects two switches, starting with the steep decay, followed by the flat regime, and finally resumption of the steep decay.

#### 4. DISCUSSION

We have identified a GRB “pulsar signature region”, within the pulsar initial parameter phase space region defined by equations (10), (11) and (12). If pulsars are associated with GRB, the afterglow lightcurves may show a distinctive, achromatic feature, namely, they flatten at a critical time  $T_c$  (eq.[6]), and steepen again at a later time  $T_{em}$  (eq.[7]). This region of pulsar parameter phase space includes “magnetars” or ultra-high field pulsars, which play a large role in some GRB progenitor models.

At present, the early afterglow data is insufficient to provide good tests for this feature. However, an interesting possibility is the achromatic bump observed in the afterglow of GRB 000301C, which for a limited time deviates significantly from the standard broken power-law fit. Possible explanations include running into a non-uniform ambient density (Berger et al. 2000), and modification by a microlensing event (Garnavich, Loeb & Stanek 2000). We suggest here a third possibility, that the bump may be caused by the pulsar signature discussed above. Taking (Berger et al 2000)  $\alpha_1 = -1.28$  for  $T < 2.5$  d and  $T > 3.8$  d, the bump index is expected to be  $\alpha_2 = 0.15$ , which seems reasonable to fit the achromatic bump. Since the feature occurs a couple of days after the GRB trigger, the initial pulsar parameters are in regime II. Taking  $E_{\text{imp},51} = 1.1$  from the observations (Berger et al. 2000), we can work out the pulsar parameters by setting  $T_{em} = 3.8$  d and  $T_c = 2.5$  d, which gives  $P_0 = 7$  ms and  $B_{p,15} = 0.55$  (Fig.1).

Another possibly relevant observation is the recent Fe line detection in the X-ray afterglow of GRB 991216 (Piro et al 2000), which may imply a continuously-injecting central engine (Rees & Mészáros 2000). If  $L_{em} \sim 10^{47}$  erg s<sup>-1</sup> is assumed 1.5 days after the burst (Rees & Mészáros 2000), this could be due to a pulsar with  $P_0 \sim 0.8$  ms and  $B_{p,15} \sim 0.15$ , which is expected to give a signature bump at somewhere between 1 hour to 16 hours. This is not seen in the afterglow light curve of this GRB (e.g. Halpern et al. 2000). However, a slightly weaker luminosity (e.g.  $L_{em} \leq 3 \times 10^{46}$  erg s<sup>-1</sup>) could still explain the Fe features, by assuming a slightly larger Fe abundance (which is low in this model). The required pulsar can then be more magnetized so that the characteristic times for the signature bump would be expected early enough to have evaded detection in this GRB.

In conclusion, the detection of or upper limits on such characteristic afterglow bumps by missions such as HETE2 or Swift may be able to provide significant constraints on magnetar GRB models and their progenitors.

We are grateful to NASA NAG5-9192 and NAG5-9193 for support, and M.J. Rees for useful comments.

#### REFERENCES

Antonelli, L.A., 2000, ApJL, in press (astro-ph/0010221)  
 Berger, E., et al. 2000, ApJL, subm (astro-ph/0005465)  
 Blackman, E. G., & Yi, I. 1998, ApJ, 498, L31  
 Blandford, R., & McKee, C. 1976, Phys. Fluids, 19, 1130  
 Chevalier, R. A., & Li, Z. 1999, ApJ, 520, L29  
 Cohen, E., & Piran, T. 1999, ApJ, 518, 346  
 Cohen, E., Piran, T., & Sari, R. 1998, ApJ, 509, 717  
 Dai, Z. G., & Lu, T. 1998a, A&A, 333, L87  
 —. 1998b, Phys. Rev. Lett., 81, 4301  
 Duncan, R. C., & Thompson, C. 1992, ApJ, 392, L9  
 Fryer, C., Woosley, S., & Hartmann, D. 1999, ApJ, 526, 152  
 Garnavich, P., Loeb, A., & Stanek, K. 2000, ApJL subm (astro-ph/0008049)  
 Halpern, J. P., et al. 2000, ApJ, in press (astro-ph/0006206)  
 Harding, A., Contopoulos, I., & Kazanas, D. 1999, ApJ, 525, L125  
 Kluźniak, W., & Ruderman, M. 1998, ApJ, 505, L113  
 Mészáros, P., & Rees, M. J. 1997, ApJ, 476, 232  
 Mészáros, P., Rees, M. J., & Wijers, R. 1998, ApJ, 499, 301

—. 1999, New Astronomy, 4, 303  
 Paczyński, B. 1998, ApJ, 494, L45  
 Piro, L., et al. Science, in press  
 Rees, M. J. & Mészáros, P. 1998, ApJ, 496, L1  
 —. 2000, ApJ Letters, in press (astro-ph/0010258)  
 Ruderman, M., Tao, L., & Klužniak, W. 2000, ApJ, 542, 243  
 Sari, R., & Mészáros, P. 2000, 535, L33  
 Sari, R., & Piran, T. 1999, ApJ, 517, L109  
 Sari, R., Piran, T., & Narayan, R. 1998, ApJ, 497, L17  
 Spruit, H. C. 1999, A&A, 341, L1  
 Thompson, C. 1994, MNRAS, 270, 480  
 Thompson, C., & Blaes, O. 1998, Phys. Rev. D, 57, 3219  
 Usov, V. V. 1992, Nature, 357, 472  
 Vietri, M. 1997, ApJ, 488, L105  
 Wijers, R., Rees, M. J., & Mészáros, P. 1997, MNRAS, 288, L51  
 Woosley, S. E. 1993, ApJ, 405, 273  
 Yi, I., & Blackman, E. G. 1998, ApJ, 494, L163

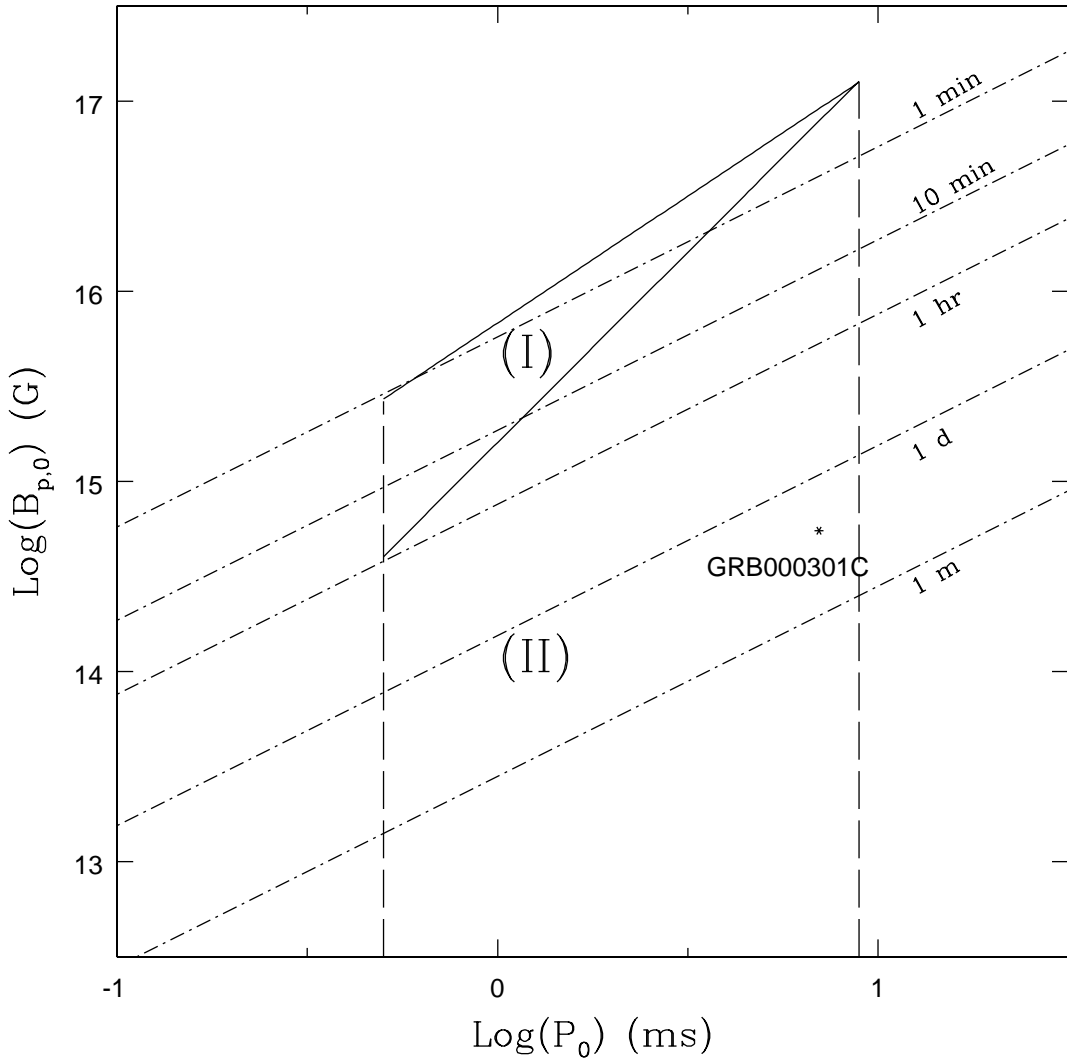


FIG. 1.— A  $B_p - P_0$  diagram for the initial parameters of a pulsar born in a GRB. The enclosed areas (regime I and II) are the phase spaces where an acromatic pulsar signature is expected in the GRB afterglow lightcurves. Dotted-dash lines denote various  $T_{em}$  expected.  $E_{imp} = 10^{51} \text{ erg s}^{-1}$ ,  $\Gamma_{0,2} = 1$ ,  $n = 1 \text{ cm}^{-3}$ , and  $P_0(\text{min}) = 0.5 \text{ ms}$  have been adopted.